Analysis of Delamination Arrest Fasteners in Bolted-Bonded Composite Structures

Wenjing Liu

A thesis

submitted in partial fulfillment of the

requirements for the degree of

Master of Science in Aeronautics and Astronautics

University of Washington

2014

Committee:

Kuen Y. Lin

Jinkyu Yang

Program Authorized to Offer Degree:

William E. Boeing Department of Aeronautics and Astronautics

University of Washington

Abstract

Analysis of Delamination Arrest Fasteners

in Bolted-Bonded Composite Structures

Wenjing Liu

Chair of Supervisory Committee:

Professor Kuen Y. Lin

William E. Boeing Department of Aeronautics and Astronautics

Delamination is one of the most critical damages in carbon fiber composites, which are being employed in primary aircraft structures. One common solution to prevent a delamination from propagating is to install fasteners, clamping the laminate together and partially arresting the delamination. In this thesis, the effectiveness of multiple fasteners installed in series to arrest the mixed-mode interlaminar failure in composite structures is investigated analytically. An accurate finite element model for predicting delamination propagation behavior of bolted-bonded structures was developed and validated by experimental test data. The finite element results showed that the presence of fasteners can slow down propagation of the crack by compressing the lamina together and transferring load via Mode II shear engagement of the fastener. Compared to the single-fastener case, damage tolerance of the structure was improved by the inclusion of the second fastener. Additionally, if the tensile modulus of the lamina is not high enough, laminate failure would occur before the delamination past the second fastener. Parametric studies were also performed to evaluate the influences of friction and laminate stiffness, fastener stiffness, fastener spacing and specimen width. Numerical results were discussed and a conclusion on the effectiveness of delamination arrest was drawn.

LIST OF FIGURES

Page

LIST OF TABLES

Page

ACKNOWLEDGEMENTS

I would like to thank my advisor, Professor Kuen Y. Lin for giving me the precious opportunity to be engaged in this project. I would also like to thank Chi Ho Cheung who provided invaluable knowledge of Abaqus and helped me a lot to debug the code. I would also like to thank Luke Richard, my best colleague, who helped me to edit the thesis. Additional thanks go to Gerry Mabson, Marc Piehl, Eric Cregger and Matt Dilligan of The Boeing Company for their discussion and suggestions. Finally, my sincerest thanks are given to my husband Kaifu, who always encourages me.

This thesis was jointly supported by The US Federal Aviation Administration (FAA) through AMTAS (Advanced Materials for Transport Aircraft Structures at the University of Washington), The Boeing Company, and Toray Composites.

Chapter 1

INTRODUCTION

1.1 Introduction

Composite materials have been developed and used in a wide variety of structural applications because of their significant improvements in specific strength and stiffness, fatigue resistance and corrosion resistance over metallic materials since the 1960s. Over the past few decades, the applications and use of carbon fiber composite has been expanded from secondary structures to their current use in primary aircraft structures.

The use of composite materials in aircraft has enabled the use of bonded (co-cured, co-bonded or secondary bonded) structures, the main advantage of which is to reduce part counts and weight. Unlike assembled structures, such integrated structures can get rid of the need for fasteners and rivets, which results in a reduction of cost and complexity associated with the legacy design approach. However, in actual aircraft structures, many discrete source damages such as impact, collision, as well as manufacturing defects can cause bonds to fail. The main damage mode in these bonded composite structures is disbond/delamination. Since these discrete damages are random and unpredictable in nature, it is likely to inflict a damage of a size that can reduce the residual strength of the structure to below the design operating load. The cracks caused by these damages will propagate along the entire bond surface when the critical load is reached. It is very dangerous for the safety of the aircraft. Therefore, there is a need for disbond arrest mechanisms in the bonded composite structures.

In aircraft structures, it is common to use fasteners for assembly of geometrically complex configurations. These fasteners are often co-located with bonded or co-cured features, and thus can also perform as disbond arrest mechanism without the added cost and complexity of alternatives such as z-pin and z-stitching. Since disbond/delamination can lead to critical failure at a structural level, it is important to understand the behavior of crack propagation and how fasteners, as disbond arrest mechanisms, interact with delamination.

Previous research by Bruun, Cheung and Lin [1-3] has shown the results of an isolated fastener to arrest the crack. It can be seen clearly that cracks may continue to propagate after it passes the fastener. Therefore, there is a need to study structures with multiple fasteners installed in series. It is also important to understand the effectiveness of these fasteners in arresting disbond to maximize their benefits and ensure safety of the structure. This thesis focus on finite element analysis of how two fasteners installed in series affects the delamination behavior of a composite structure.

1.2 Objective

The objective of this thesis is to develop an effective and stable accurate finite element tools to predict crack propagation behavior of bonded structures with two fasteners installed in series and conduct research to extend prior research by Lin to investigate the capability of double-fastener model to arrest and stabilize crack propagation in composite structures.

1.3 Background

1.3.1 Virtual Crack Closure Technique (VCCT)

One of the most critical failure modes for composite structures is disbond/delamination [4-6]. The remote loadings applied to composite structures are typically resolved into interlaminar tension and shear stresses at discontinuities that create mixed-mode I, II and III delaminations. To characterize the onset and growth of these delaminations, the use of fracture mechanics has become common practice over the past two decades [7-9]. The total strain energy release rate, G_{total}, the mode I component due to interlaminar tension, G_I, the mode II component due to interlaminar sliding shear, G_{II}, and the mode III component, G_{III}, due to interlaminar scissoring shear, as shown in Figure 1, need to be calculated. In order to predict delamination onset or growth for two-dimensional problems, these calculated G components are compared to interlaminar fracture toughness properties, G_c, measured over a range from pure mode I loading to pure mode II loading. Failure is expected when, for a given mixed mode ratio G_{II}/G_{total}, the calculated total energy release rate, G_{total}, exceeds the interlaminar fracture toughness, G_c [10].

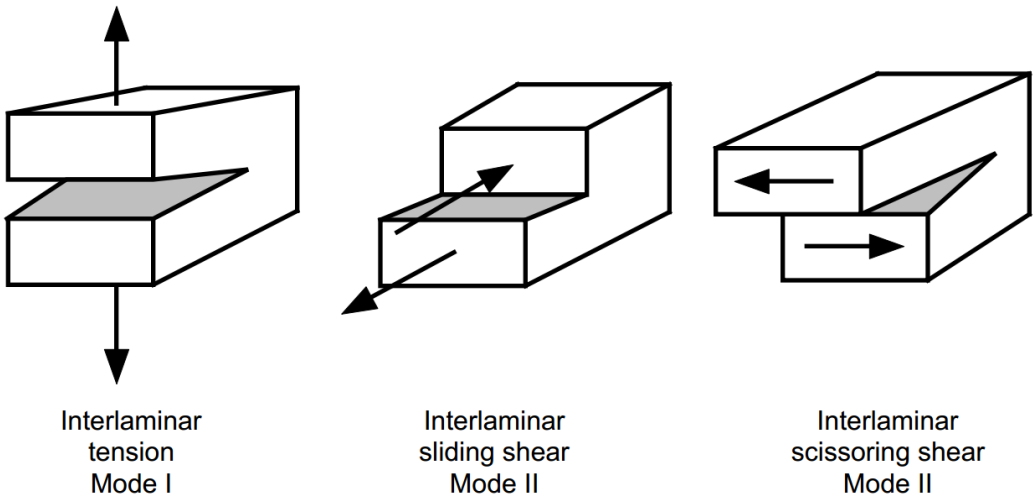

Figure 1.1 Fracture Modes

A variety of methods are used to compute the strain energy release rate based on results obtained from finite element analysis. The finite crack extension method, which is based on Irwin's crack closure integral [11, 12], requires two complete analyses. The method is based on the assumption that the energy ΔE released when the crack is extended by Δa from a to $a+\Delta a$ is identical to the energy required to close the crack. The modified, or virtual, crack closure method, proposed by Rybicki and Kanninen [13], is based on the same assumptions as the crack closure method described above. Additionally, however, it is assumed that a crack extension of Δa from $a+\Delta a$ to $a+2\Delta a$ does not significantly alter the state at the crack tip. Therefore the virtual crack closure technique is a one-step method. It calculates the individual SERRs from a single FE analysis. [Lyle et al. 14] implemented the VCCT in commercial FE code ABAQUS in the form of interface fracture element. Qian and Xie [15] extended the interface element for analysis of dynamic crack propagation.

Research has also been conducted on the determination of SERRs using analytical methods. Based on classical plate theory, Schapery and Davidson, and Suo and Hutchinson [16] developed an analytical crack-tip element. Only two loading parameters, the crack tip force and moment, are needed in this method. They are both analytically determined using plate theory. However, this method provides one total strain energy release rate. Mode decomposition can only be carried out with the aid of a mode-mix parameter, which is determined either by experiments or

an additional finite element analysis. Wang and Qiao [17] extended the work based on a novel shear deformable bi-layer beam theory and rotational flexible joint deformation model, which yield the closed-form solution to the mode-decomposed SERRs for an interface crack in layered composite plate structures.

1.3.2 Implicit Fastener Modeling

The implicit modeling of fasteners as simple structural elements, such as rods, springs, has also been an area of interest in the industry due to its computational efficiency. Models of fastened joints can be assembled with only a few plates (in 3-D model)/beams (in 2-D model) and fastener elements. Morris [18] recently made a review of a number of fastener flexibility formulae, in which the in-plane flexibility of the joint is expressed by only a joint compliance/stiffness value. Tate and Rosenfeld [19] proposed a conclusion based on multi-fastener metallic symmetric butt joints. It is said that the total fastener compliance can be calculated as the sum of four individual compliances: fastener shear, fastener bending, fastener bearing, and plate bearing. Huth [20] subsequently developed an empirical expression for fastener compliance of multi-row single and double lap joints. This expression was derived from a large number of experimental datasets and is valid for bolted metallic joints, riveted metallic joints, and bolted graphite/epoxy joints. Huth stated that his solution provided higher accuracy compared to previously existing expressions. Rutman and Kogan [21] developed a FE modeling approach for fastener joints using implicit fastener elements, in which both in-plane flexibility and bending interactions are considered. There are numerous similar methods and techniques developed for the similar purpose to efficiently solve the loads transferred by fasteners, in order to predict the static and fatigue strength of the joints.

1.3.3 Hybrid Bolted Bonded Joining Technology

The subject of the current research shares the closest resemblance to the hybrid bolted bonded joining technology in lap joints, originally presented as a fail-safe concept by Hart-Smith [22] in 1985. Kelly [23] conducted several experiments and showed that hybrid joints can have a greater static and fatigue strength than bonded joints. However, analyses of these joints often rely on

explicit modeling with finite element method. Recently, Barut and Madenci [24] developed a semi-analytical solution method for stress analysis of single-lap hybrid bolted-bonded joints. This method permits the determination of point-wise variation of displacement and stress components and the bolt load distribution in the joint.

Chapter 2

FINITE ELEMENT MODELING

A simplified 2-D model of the fastener crack arrest mechanism, as shown in Figure 2.1, is used to evaluate the effectiveness of the fasteners as a crack arrest mechanism. The model is discretized and the crack propagation is numerically simulated in commercial finite element software, Abaqus. Crack propagation is simulated using the Virtual Crack Closure Technique (VCCT). The fastener is reduced to two independent spring elements; the stiffness of the fastener shear joint is calculated using the fastener flexibility approach by Huth.

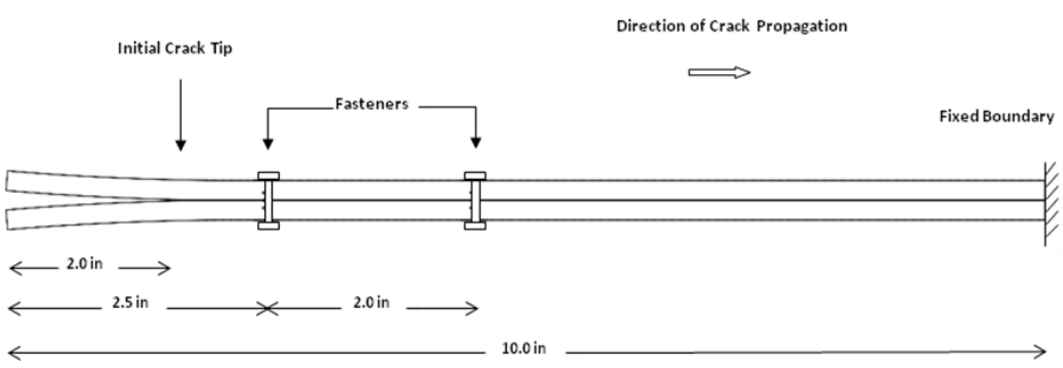

Figure 2.1 The 2-D Schematic of Fastener Crack Arrest Mechanism

2.1 Description of Initial Finite Element Model

Based on the prior single-fastener model successfully designed by Bruun, Cheung and Lin [1-3], the model used in the study comprises of an upper plate and a lower plate which depict a delaminating skin/string system in the aircraft structures. Identical 24-ply symmetric, balanced laminate layups are used for both upper and lower plates. The choice of identical, symmetric and balanced layups is to eliminate any strain energy release rate caused by differential thermal expansion and tension-bending coupling; and the increase in the number of plies from 16 (used in previous a single-fastener model designed by Cheung [3]) to 24 is to guarantee that the laminate failure would not occur before the crack propagation. The layup used are (45/0/-

$45/90)_{3s}$ with 25% 0° plies. The crack is located at and confined to an infinitesimally thin matrix interface between the upper and the lower plates; the crack tip is confined to the 90/90 interface and crack bridging is not modeled. In general, bridging would result in an apparent increase in the critical strain energy release rate/fracture toughness and would be an optimistic scenario. A finite thickness bond layer is not explicitly modeled; it is assumed that crack propagation occurs whenever the critical strain energy rate is reached, regardless of bond type (co-cured, co-bonded or secondary bonded) or fracture failure type (cohesive failure or adhesive failure). The mode-decomposed energy release rates are evaluated using the VCCT, implemented in Abaqus FEA software. A mixed-mode fracture law, B-K law, is used to determine crack propagation behavior. Only static crack propagation is considered.

The modeling of the fastener is simplified to two independent springs; one representing the axial stiffness of the fastener and one representing the shear stiffness pertaining to a bolted joint. The relative rotation of the mechanically fastened plates is assumed to be small. The shear stiffness of the bolted joint is obtained using the fastener flexibility approach. The next section will detail how to calculate these stiffness properties. Specifically, the sliding spring is hooked up in a way deliberately to generate a moment when loaded; they are connected to the lower surface of the top plate and upper surface of the lower plate. Additionally, in order to deliver the spring force distributed through the thickness, a "fastener wall" is modeled as beam elements.

The model is 10 inches long. The initial crack is 2 inches long. The first fastener is located 2.5 inches from the cracked end. The second fastener is typically located 4.5 inches from the cracked end, which provides a 2-inch fastener spacing. The initial 0.5 inches of crack propagation is not influenced by the fasteners/springs and is only driven by the external loads. As the crack propagation passes the fasteners/springs, the springs react to the crack opening displacements and provide resistance to propagation.

Loads are applied to the cracked end of the plates, while the intact end is given fixed boundary conditions. In general, any combination of moments and axial forces can be applied to the plates. In this study, a pure Mode I load case (symmetrically applied opening moment) and a mixed-mode load (tension applied to the lower plate) are used. These load cases are chosen because

they can best demonstrate the effectiveness of fasteners in arresting propagation and represent configuration that could be tested in laboratory environments.

2.1.1 Properties

The lamina properties used are modeled after the T800/3900 material system; they are summarized in Table 2.1. A mixed-mode fracture law, B-K law (Equation 2.1), is used to determinate crack propagation behavior. In general, the fracture parameters are dependent on a multitude of factors, e.g. the lamina orientations that bound the crack, process quality, the presence of bridging, and the type of bond failure if a bonded structure id considered. However, for the purpose of this study, a single set of independent parameters is assumed.

$$G_{equivC} = G_{IC} + \left(G_{IIC} - G_{IC}\right)\left(\frac{G_{II}}{G_I + G_{II}}\right)^{\eta} \tag{2.1}$$

Table 2.1 Composite Lamina Material Properties

Ply Thickness	0.0075 in
E_1	19.6×10^6 psi
$E_2=E_3$	1.13×10^6 psi
$G_{12}=G_{13}$	0.580×10^6 psi
G_{23}	0.369×10^6 psi
$\nu_{12} = \nu_{13}$	0.34
ν_{23}	0.53
G_{IC}	1.6 lb/in
G_{IIC}	14 lb/in
η	1.75

A Titanium fastener made of Ti-Al6-V4 with an elastic modulus of 16.5 Msi is used in the model. The axial property of the fastener is calculated assuming it is a constant diameter bar. The shear stiffness of the fastener joint modeled using the fastener flexibility approach. The flexibility of the un-bonded bolted joint in the shear direction, C, is given by equation (2.2). The parameters used are: t_i = laminate thickness, d = fastener diameter, n = single or double shear joint, $E_{1/2}$ = laminate stiffness, E_3 = fastener elastic modulus, constant a = 2/3 and b = 4.2 for bolted graphite/epoxy joints.

$$C = \left(\frac{t_1 + t_2}{2d} \right)^a \frac{b}{n} \left(\frac{1}{t_1 E_1} + \frac{1}{n t_2 E_2} + \frac{1}{2 t_1 E_3} + \frac{1}{2 n t_2 E_3} \right) \tag{2.2}$$

The properties of the materials and structural members are assumed to be linear elastic. No failure points are defined except for the criteria for static crack propagation. In general, the failure envelope should include many competing failure modes, such as tension failure, bending failure, fastener shear-off, fastener pull-through, etc. However, for the purpose of this study, only static crack propagation is considered. With an exception, “free-play” and “preload” is optionally added to the fastener flexibility and stiffness as nonlinearity. This is to simulate the effect of fastener hole tolerance and fastener install torque present in composite structures.

2.1.2 Finite Element Model

The 2-D finite element mesh of the model is constructed in Abaqus FEA software, shown in Figure 2.2. The plates are 10 inches long and 0.18 inches thick. The width is 1.25 inches, providing a width-to-diameter ratio of five using a 0.25 inches diameter fastener. The CPE4R 2-D 4-node bilinear quadrilateral plane strain element with reduced integration is used in the plates. One element represents one ply thickness of 0.0075 inches; each element is approximately 0.0075 inches in length, yielding a length-to-height ratio of approximately one. The mesh size is kept constant in order to maintain a consistent accuracy level for VCCT solutions as the crack propagates along the length of the model. This mesh size also ensures the convergence of VCCT and global displacement solution. The initial crack is 2.0 inches long. Two fastener springs are attached to the plates 2.5 inches from the cracked end as the first fastener; the other two fastener

springs representing the second fastener are attached to the plates 4.5 inches from the cracked end. Specifically, the shear springs are attached to the lower surface of the upper plate and the upper surface of the lower plate to simulate the coupling moment reacted by the plates. A spring (clamp spring) with preload is used to model the fastener install torque; a nonlinear spring (shear spring) with free-play is used to model positive fastener hole clearance. Additionally, beam elements (B21) are established as fastener wall to simulate the distribution of spring force through the thickness. The fastener wash/nut is modeled as beam elements (B21), as well.

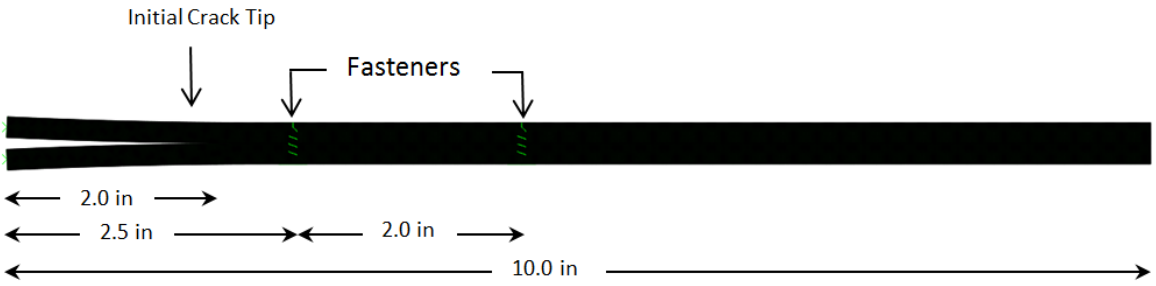

(Deformed under Mode I Loading)

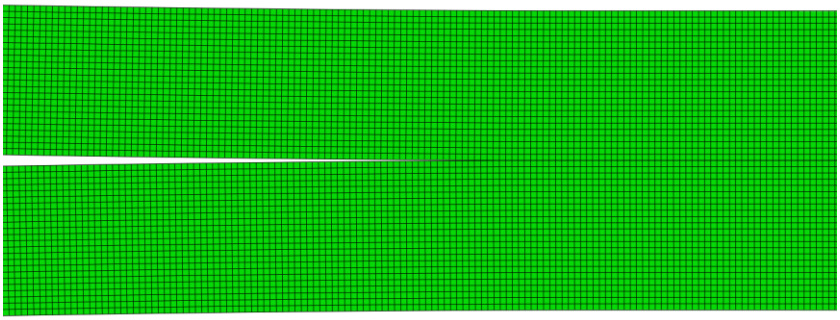

(Enlarged Near the Crack Tip)

Figure 2.2 Finite Element Mesh

The two plates are tied to each other along the surface, with the exception of the initial crack, to model the intact portion of the structure. The tied surface also defines the interface at which the crack will propagate along. The mode-decomposed SERRs are evaluated using the VCCT elements positioned along the crack interface. The SERR for each mode is calculated separately

using the nodal forces at the crack tip and the opening/sliding displacements behind the crack tip. The tie condition applied to the crack tip is released when the mixed-mode fracture criterion (Equation 2.1) is satisfied, and the crack propagates to the next node. The cracked surface is then given a contact condition with the desired friction coefficient. The crack propagates in the FEA environment in a node-to-node fashion regardless of the stability of the propagation. It means, for example, an unstable propagation would result in all the interface nodes releasing sequentially but at the same applied load, since the simulation is load-controlled.

The crack propagation simulation consists of many individual static equilibrium steps. The steps are needed in order to update the global matrix for nonlinear geometric effects, and to update the geometry every time the crack propagates forward.

2.2 Sensitivity to Fastener Wall Modeling

The initial model has only been validated by single-fastener case. In this study, a second fastener is added as the continuation of the single-fastener crack arrest mechanism study. Therefore, after the initial model was created and a consistently convergent solution was obtained, further refinements were required to improve the accuracy of the predicted response due to the inclusion of the second fastener. Since the mode I component had been shut down as the crack propagates pass the first fastener, the load increase required to propagate the crack due to the second fastener was expected to be equal or even less than the load increase at the first fastener. However, it did not seem to be the case. The predicted crack arrest capability of the second fastener obtained from the finite element model was significantly larger than what was expected, as shown in Figure 2.3. The second fastener is approximately two times more effective than the first fastener.

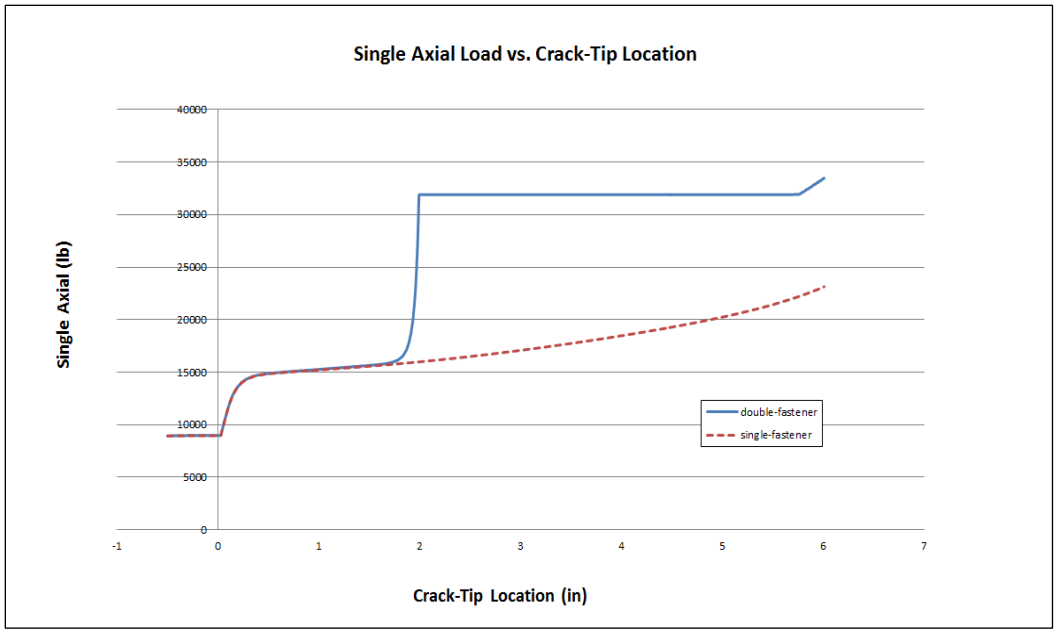

Figure 2.3 Result of Initial Finite Element Model

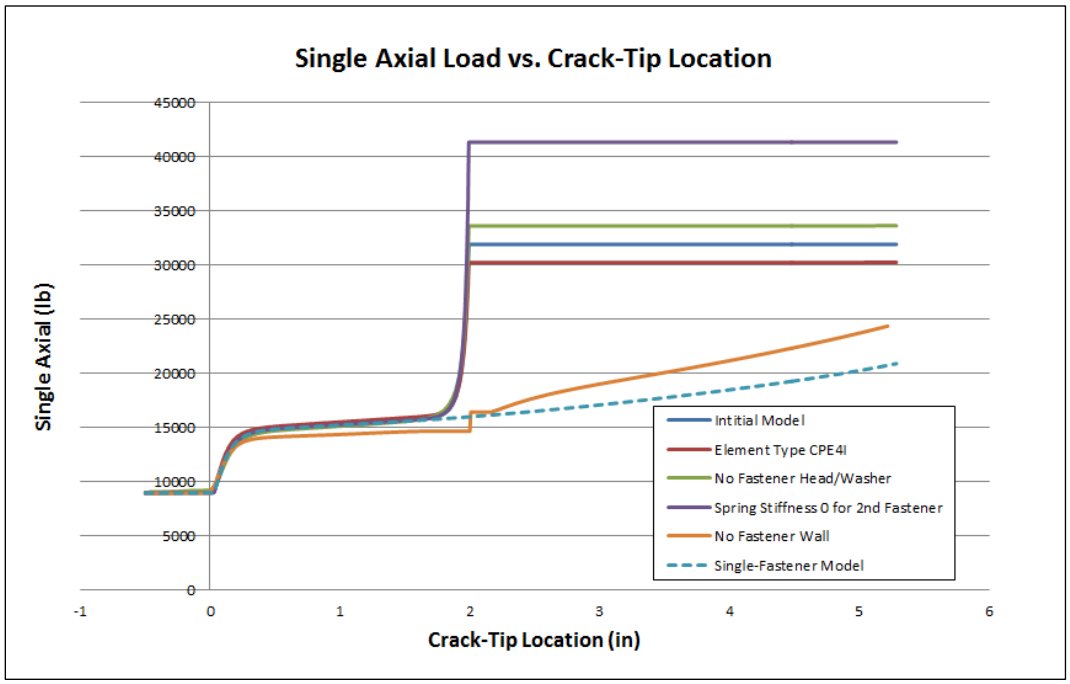

Figure 2.4 Results of Different Trial Models

There are two probable explanations for this interesting phenomenon: one being modeling error; the other one being beneficial interaction between the two fasteners. In order to figure out the real reason, several extra models with different element types or different spring stiffness values were developed. All the results are shown in Figure 2.4. Finally, it was concluded that this inaccurate and unreasonable result was caused by the modeling methodology of the shear property of the fastener. Interestingly, it did not affect the results of single-fastener finite element model.

2.3 Modification of Fastener Modeling

The model of each fastener system used in previous research on the propagation characteristics of disbond/delamination in specimens with one arrest fastener conducted by ChiHo Cheung comprises of four parts: two independent springs, a fastener wall and a fastener head. The two independent springs represent the axial/clamp stiffness and the shear/slide stiffness of the fastener respectively. The sliding spring is hooked up in a way to generate a moment when loaded; it is connected to the lower surface of the top plate and the upper surface of the lower plate. There are a many elements through the thickness, but the spring is only connected to the lowest element. Therefore, the spring force is only delivered to the lowest node rather than distributed through the thickness, whereas with a real fastener interacting with a fastener hole wall, the forces would be distributed along among the contact surface. This is the reason why the fastener wall is modeled. The fastener wall is modeled as 2-D 1st-order interpolation beam element, B21, with zero Young's modulus and infinity shear modulus. It ties a bunch of nodes through the thickness so that the spring force can be distributed through the thickness and preserves the reaction moment from the fastener joint. The fastener head is a separate thing for simulating the fastener head/nut with washer. Since all the clamp spring force applied to one node, a singularity exists and that results in incorrect G_I, G_{II} at the crack tip. The presence of fastener head spreads out the forces, takes away some local spiking, and makes convergence easier in most cases. The fastener head is also modeled as beam element (B21), the property of which is determined by using equivalent stiffness methods.

2.3.1 Removal of Fastener Wall

While successful in single-fastener model, the methodology for modeling arrest fastener system described above did not work anymore in the double-fastener specimen. The presence of fastener wall, which was designed to distribute the shear/slide spring force through the thickness of the plates, led to an artificial spike of propagation load at the location of the second fastener. This was because the fastener wall beam increased the local shear stiffness of the laminated plates at the point of the fastener, which contradicts the reality. The removal of the fastener wall reduced the propagation load spike at location of the second fastener immediately by 70% to a reasonable level, as shown in Figure 2.5.

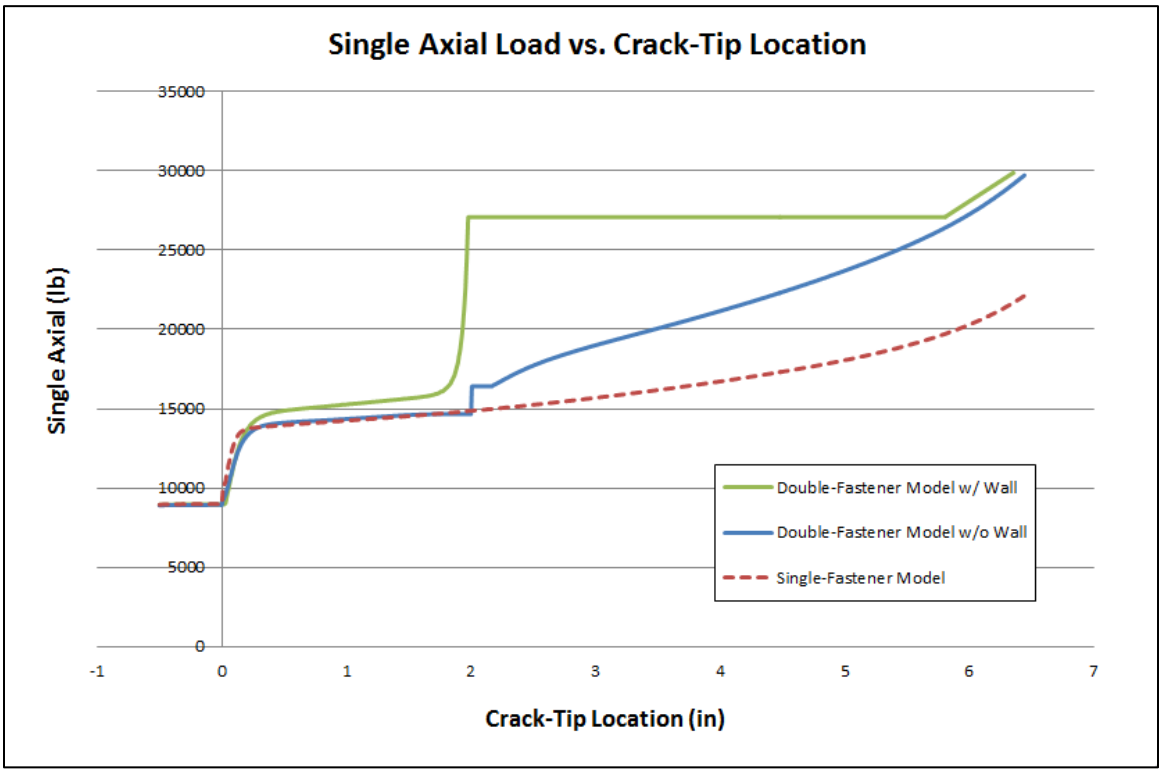

Figure 2.5 Result of Revised Model without Fastener Wall

2.3.2 Modification of Sliding Spring Location

Although the removal of the fastener wall reduced the unreasonable load spike at the second fastener effectively, the steep jump in load still remained there, as seen in Figure 2.5. Further investigation indicated that the node connected to the shear/sliding spring showed excessive deformation, while the neighboring nodes lagged behind, as shown in Figure 2.6, which resulted in a singularity problem at the nodes of interest. This finally led to a softer joint and questionable the G_{II} estimates.

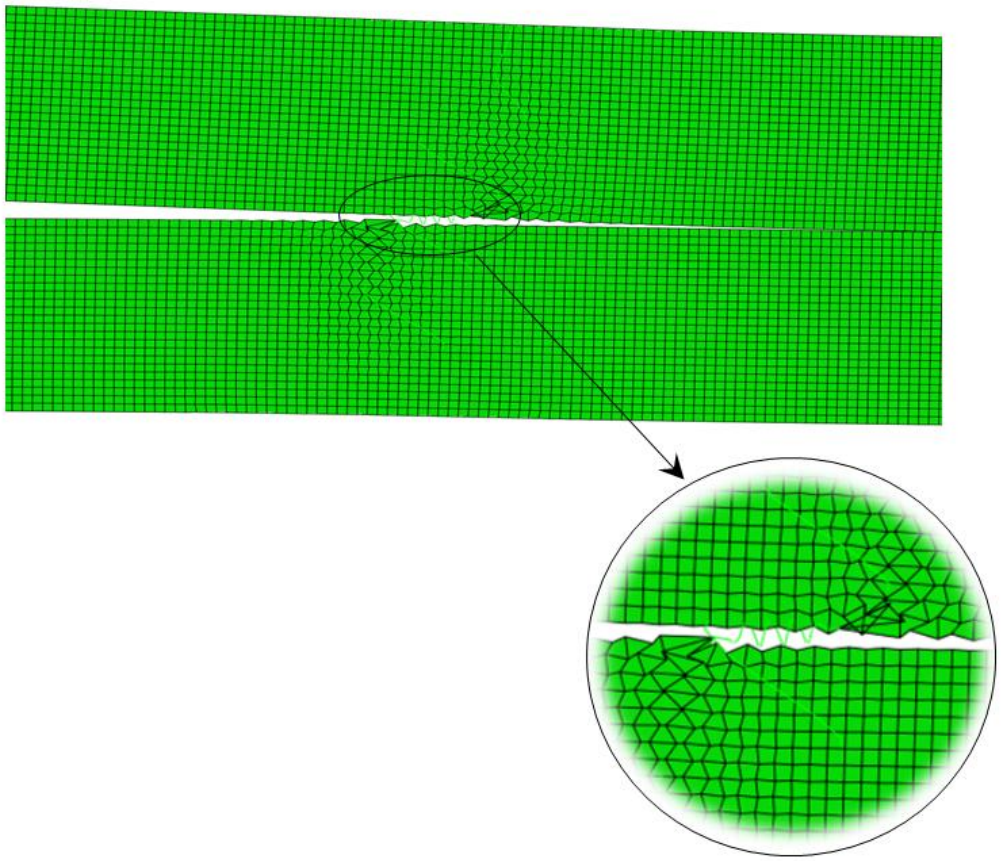

Figure 2.6 Deformation of the Nodes around the Fastener Area

To solve the above-mentioned singularity problem, the shear/sliding spring was moved 1 element off the interface/bondline of the model. The result is demonstrated as Figure 2.7. It can be seen clearly that the steep jump of the propagation load was eliminated, and a more realistic

and reasonable response was obtained. Furthermore, it is noted that with the inclusion of preload, the step increase in propagation load due to mode transition occurs before the crack tip reaches the first fastener, due to the elastic influence of the fastener generated by the preload. However, since the crack propagates in pure Mode II after it passes the first fastener, the second fastener has only one arrest mechanism, i.e. fastener joint resistance, providing the arrest capability. This resistance should only occur when the crack tip hits the centerline of the fastener. Therefore the load increase at the location of the second arrest fastener always occurs after the crack tip propagates past the fastener, no matter if the preload is included or not.

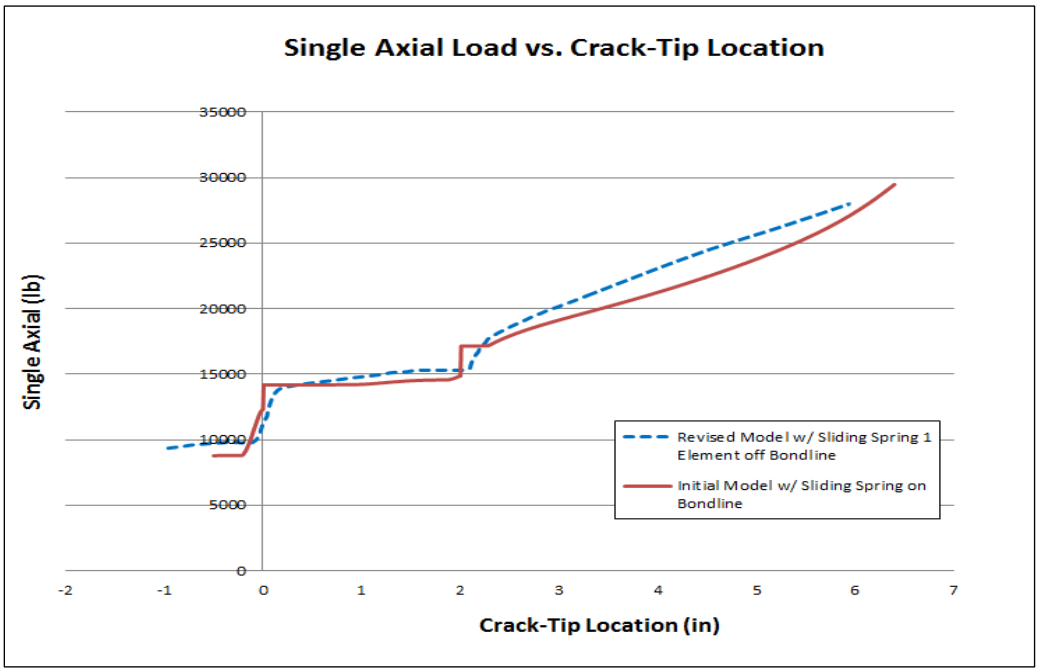

Figure 2.7 Result of Revised Model with Improved Sliding Spring Location

2.4 Results and Discussion

2.4.1 Effect of Fastener under Mode I Loading

Mode I is generally the most problematic fracture mode because G_{IC} is much lower than G_{IIC}. The opening mode is also allows moisture and contaminations to seep into the crack tip, which will exacerbate the damage. The mechanics of crack arrest with two fasteners under Mode I loading is easily understood. Nonetheless, the simple case of pure Mode I loading is discussed here for completion.

Figure 2.8 shows the applied moment vs. crack-tip location for the model with and without fasteners. The first fastener is positioned at crack-tip location zero while the second fastener is at crack-tip location two. Without the fasteners, the crack propagation is unstable. This is because applied moments produce a constant G_I at the crack tip regardless of crack-tip location; therefore crack propagation is catastrophic once the critical load is reached. It can be seen clearly that the growth of the crack is extremely well arrested by the first fastener, as expected. The loads required for propagation exponentially increase and reach asymptotic values while the crack stops within one fastener head/washer diameter from its location. The crack is completely arrested because the pivot provided by the fastener actually results in a closing moment at the crack tip. It can also be observed that the required load increases before the crack tip reaches the centerline of the fastener because of the wider elastic influence of the fastener on a bending plate. Additionally, one would observe that the apparent G_{IC} value increases from the material G_{IC} to infinity as the crack passes the fastener. The ultimate failure mode under Mode I loading would likely be laminate failure in bending or fastener pull-through.

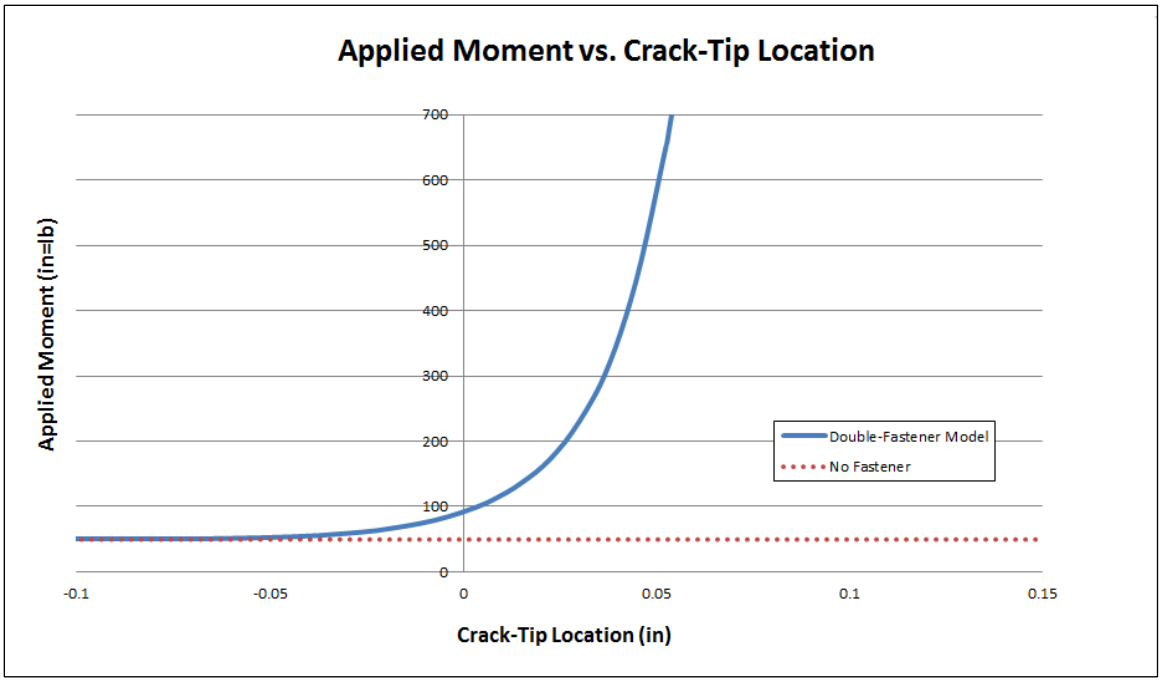

Figure 2.8 Propagation Load vs. Crack-Tip Location in Mode I Loading

2.4.2 Effect of Fastener under Mixed-Mode Loading

In general, bonded/co-cured structures experience in-plane multi-axial operating loads, which are Mode II in nature. However, when a large crack develops in the structure, load eccentricity and local buckling result in a Mode I component being added to the crack tip. This is especially acute for features such as stringer/spar terminations where the peel stress is high. The presence of even a small amount of G_I can significantly reduce the propagation load, and thus the safety of integrated structures.

The effectiveness of the fasteners in a mixed-mode load case is also studied. Friction between surfaces is not considered here. The mixed-mode load case is created by applying axial tension to the cracked end of the lower plate. It should be noted that due to the finite dimensions of the FE model and large geometric deformations, while the external load case remains the same, the fracture mode-mixity will change as the crack propagates along the bondline of the two plates. Figure 2.9 illustrates the results. The crack behavior before reaching the second fastener is

consistent with the previous single-fastener specimen. This means the second fastener does not contribute to the pre second fastener crack propagation at all.

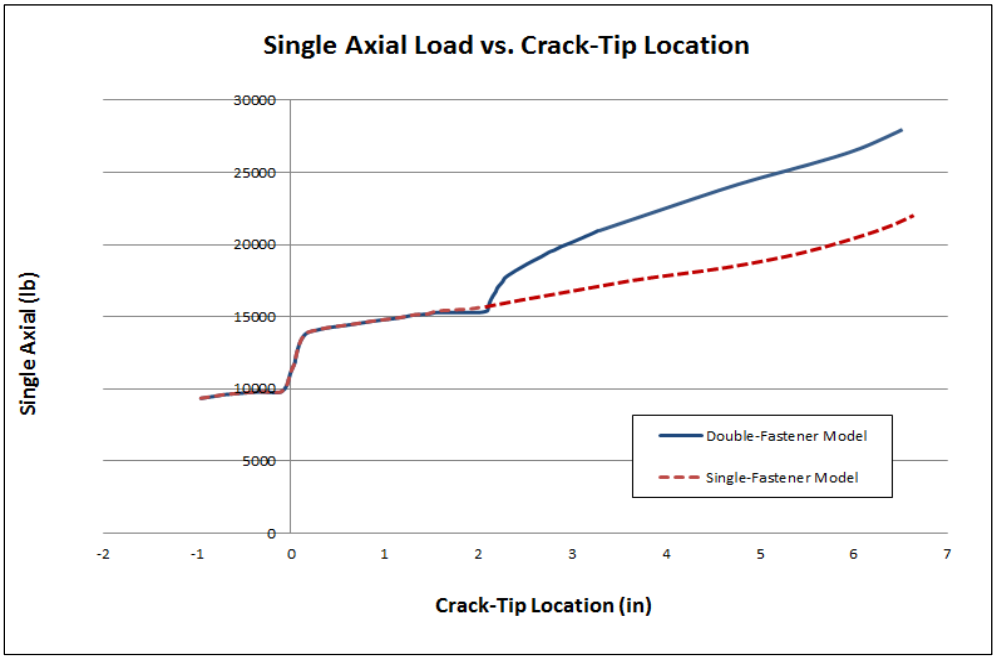

Figure 2.9 Propagation Load vs. Crack-Tip Location in Mixed-Mode

The initial crack begins to propagate unstably as the critical load (8,777lb) is reached. At this stage, the crack tip is under mixed mode condition, but dominated by Mode I. When the crack tip jumps to the first fastener's influence area, it is arrested or retarded by two different mechanism acting together: one being Mode I suppression, as shown in Figure 2.10, which forces G_{II} to increase to make up for the loss of G_I; the other being the straight-forward elastic resistance provided by the fastener joint. Ultimately, Mode II load becomes what drives the crack to go down the specimen and the crack propagation transitions to a new phase called "stable propagation" phase (Figure 2.11) until the crack tip hits the second fastener. The "stable propagation" phase begins when the crack tip reaches about 0.18 inches past the fastener centerline. In this phase, the propagation load is only resisted by the stiffness of the fastener joint (without consideration of friction).

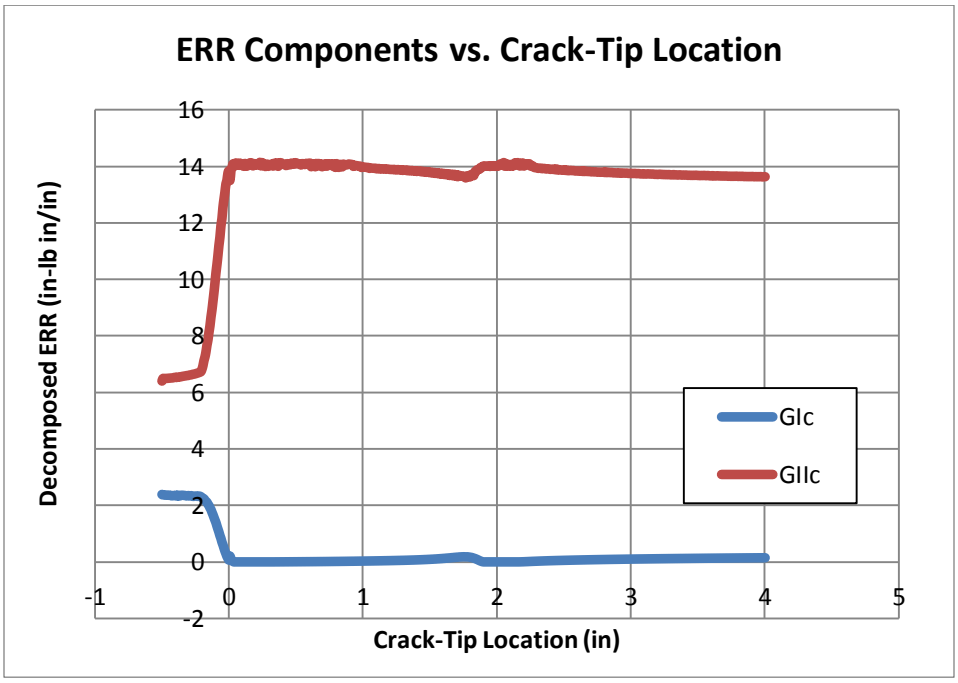

Figure 2.10 SERR Components vs. Crack-Tip Location in Mixed-Mode

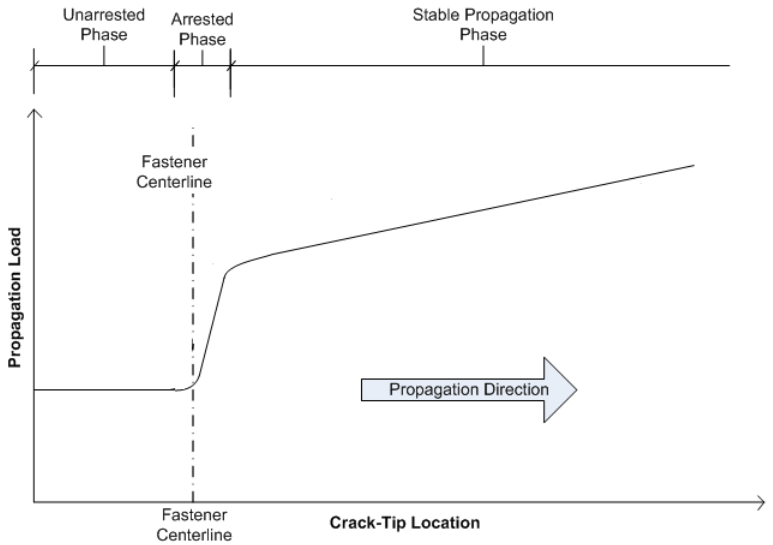

Figure 2.11 Crack Propagation Behavior with Arrest Fastener

The arrest effectiveness of the second fastener is approximately 50% of that of the first fastener. The reason is that fracture mode transition is no longer exist at the second fastener, therefore

there exists only one arrest mechanism, i.e. fastener joint resistance, providing the arrest capability. It is also obvious from the Figure 2.10 that the crack propagation past the second fastener is more stable than that past the first fastener. It is thought that this is due to different fastener joint stiffness since the crack propagation stability is provided by the fastener joint load path, the property of which is quantified by the fastener flexibility. When the crack tip goes past the second fastener the equivalent fastener joint stiffness could be treated as the two fasteners connected in parallel.

Additionally, further analysis shows that strong crack-face friction generated by fastener install preload has a significant effect on crack arrest; however, fastener-hole clearance could limit the performance of the arrest mechanism by delaying the engagement of the fastener joint.

2.4.3 Comparison of FE Modeling and Experimental Results

Figure 2.12 shows the comparison of the finite element analytical result and experimental results. The Abaqus VCCT model correlated reasonably well with the test, showing similar load jump and crack propagation rate. The most significant difference between them is that the test shows a slight shift of the curve to the right. This is due to the fact that the crack-tip location is only observed from the edge of the specimen; however, the crack front is expected to curve around the fastener, forming a V-shape. As a result, the crack-tip locations observed from the edge are greater than that obtained from the FE model, especially near the vicinity of the fastener. The other difference is that the FEA predicted load is slightly higher than test result. The author suggests the cause is three unknown factors: 1) contact friction between the upper and lower plates; 2) fastener hole clearance; 3) fastener flexibility approach.

In general, the Abaqus finite element modeling provides a satisfactory capability for predicting the crack propagation behavior in laminated composite structures with arrest fasteners installed in series. Both the experiment and the FE analysis demonstrated the effectiveness, as well as the necessity, of utilizing arrays of crack arrest fasteners. Similarly, using paralleled arrays to cover a wider crack front should also be feasible to some degree.

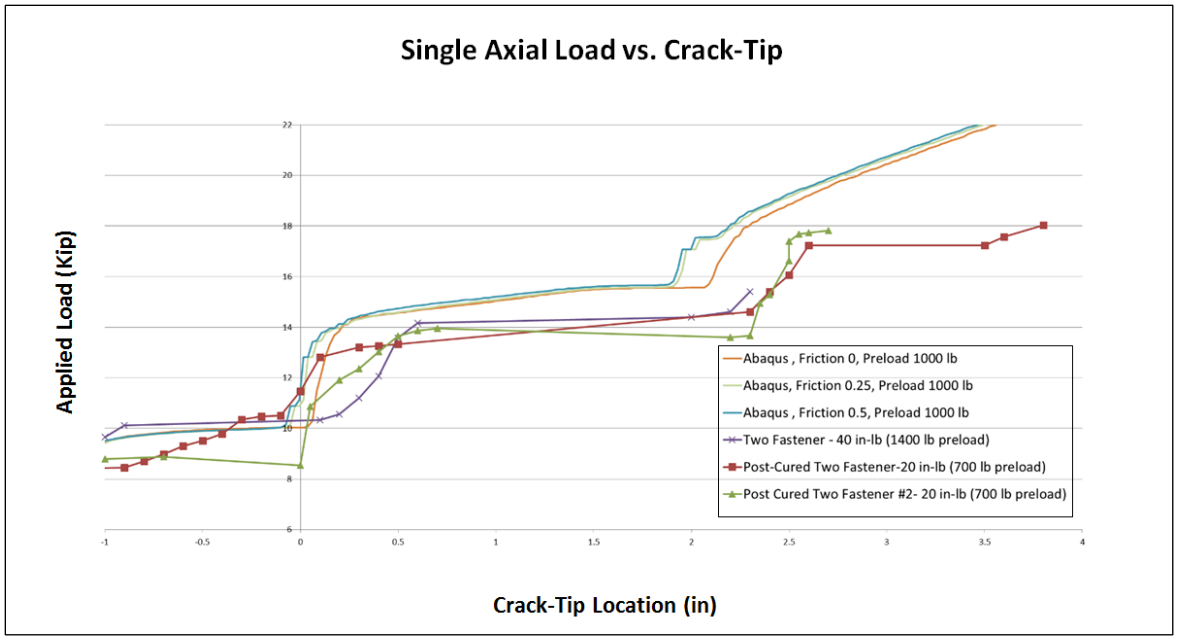

Figure 2.12 Comparison of FE Modeling and Experimental Results

2.4.4 Comment on Alternate Failure Modes not Considered in the Current Model

The primary purpose of the fastener arrest mechanism is to make sure that the delamination can be arrested so that the damage is contained and the load bearing capability of the surrounding structures is safeguarded. This statement can be quantitatively ambiguous, because the analyses show that the crack could potentially propagate indefinitely provided unlimited load, without realistic alternative failure modes defined. However, the arrest mechanism only needs to stand up to the punishment until something else fails, that is, alternate failure modes such as laminate failure, fastener failure and bearing failure. Therefore, the consideration of these alternate failure modes would provide a realistic bound to the analyses presented in the research. A designer would have to employ the crack arrest analysis in conjunction with the analyses for the alternate failure modes in order to determine the optimal design.

Chapter 3

PARAMETRIC ANALYSIS USING THE FE MODEL

With the finite element model validated by the test, parametric study can be performed. The purpose of the parametric study is to investigate the effect of changing several properties (e.g. laminate layups, fastener diameter, friction coefficient) on fastener arrest behavior of composite structures. The result of the parametric study will provide information for further optimization using fastener arrest mechanism. All parametric analyses vary from a base configuration. The base configuration parameters of previous model designed in last chapter are summarized in Table 3.1.

In general, the failure envelope would include many competing failure modes, such as laminate failure, fastener failure, etc. Therefore, the consideration of these alternate failure modes would provide a realistic bound for optimization. A designer would have to employ the crack arrest analysis in conjunction with the analyses for the alternate failure modes in order to determine the optimal design.

Table 3.1 Base Configuration Parameters

Parameter	**Value**
Laminate layup	$[(45/0/-45/90)_3]_s$
Laminate thickness	0.18 in
Specimen width	1.25 in
G_{IIC}	14 lb-in/in^2
Fastener diameter	0.25 in
Fastener spacing	2.0 in
Fastener flexibility	$6.22*10^{-6}$ in/lb
Fastener preload	3600 lb
Friction coefficient	0

3.1 Variation of Laminate Stiffness

The essence of optimization of composite design is choosing the right orientation angle to acquire best laminate properties. As a result, the effect of variation of laminate stiffness on fastener arrestment behavior for bolted bonded structures was of particular interest. The stiffness was simply varied by changing the layups only. The number of plies in each case kept unchanged, that is, 24, which provided a constant thickness. The stiffness of both the upper and lower plates was varied at the same. The layup variations are shown in Table 3.2.

Table 3.2 Parametric Analysis Layups

Layup	Layup percentage
$[45/90/-45/0/-45/90/45/90/-45/0/45/90]_s$	[17/50/33]
$[(45/0/-45/90)_3]_s$	[25/50/25]
$[45/0/45/90/45/0/-45/0/45/0/-45/90]_s$	[33/50/17]
$[(0/45/0/-45/0/90)_3]_s$	[50/33/17]

Figure 3.1 shows the effect of changing laminate stiffness. It can be seen that an increase in the laminate stiffness increases the load required to propagate the crack. This characteristic can be traced to the "pre-arrestment" phase, where the initial crack just begins to propagate and the fastener arrest mechanism has not impacted the system. The capability of arrest fastener seems to be similar for laminated plates with different stiffness. At the first fastener, which is positioned at the crack-tip location zero, the load increase for each of the trends is approximately 4,000 lbs. At the second fastener, that is positioned at the crack-tip location two, the load step decreases slightly as the laminate stiffness increases.

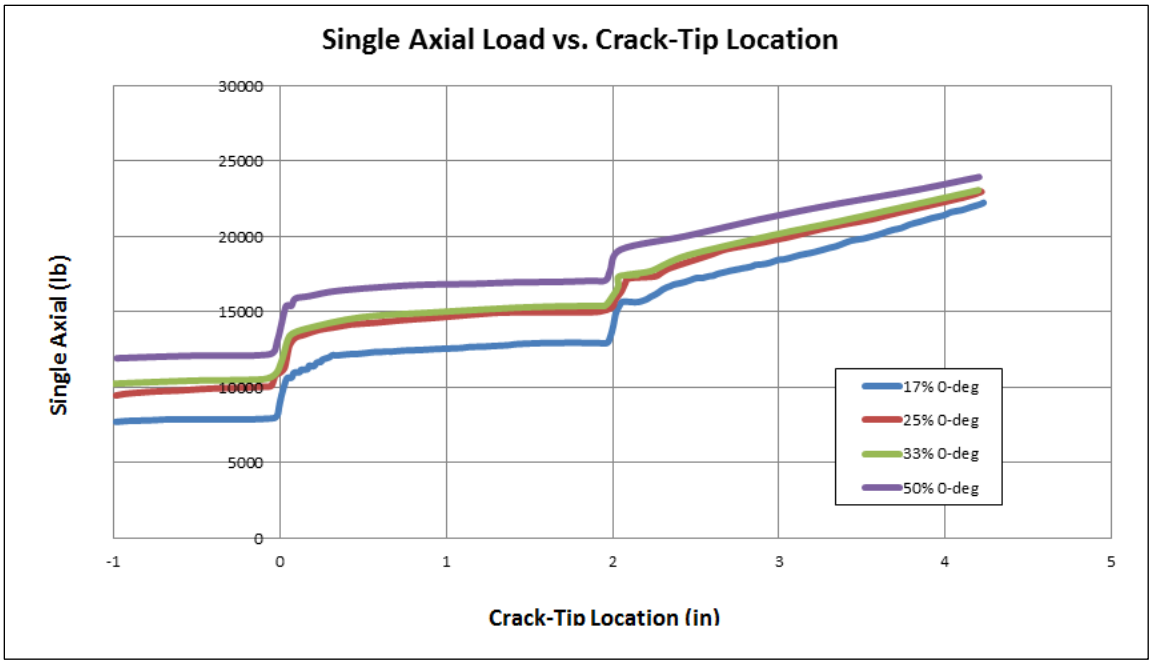

Figure 3.1 Propagation Load for Varying Layups

3.2 Variation of Specimen Width

Both finite element analysis and lab testing show that a second fastener will shift the failure mode away from delamination once the crack tip reaches the second fastener. The fastener joint resistance transfers the propagation load. Therefore, the addition of the second fastener is highly recommended. However, with the addition of the second fastener, laminate failure would occur before the crack completely passes the second fastener. This would necessitate the increase of specimen width to guarantee that the disbond/delamination will still be the ultimate damage mode. One the other hand, variation of specimen width actually provides variation of width-to-diameter ratio, which is an important factor in optimization design. Table 3.3 summarizes the width variations.

Table 3.3 Specimen Width Variation Values

Specimen width	Width-to-diameter ratio
1.25 in	5
1.5 in	6
2.0 in	8
2.5 in	10

Figure 3.2 shows the effect of varying the specimen width from the base configuration (1.25 inches). From the plot it can be seen that the fasteners in wider specimen are less effective than those in narrower specimen. A decrease in specimen width, equivalently a decrease in width-to-diameter ration, results in higher load step in "arrested phase" (Figure 2.11) and more stable crack propagation in "stable propagation phase" (Figure 2.11). The reason for this is easily understood if 3-D model is developed. In order to explain this phenomenon, results observed in experiment are employed. As shown in Figure 3.3, when the crack propagates around the fasteners, the crack front forms a "V-shape" centered on the fastener. That means the effectiveness of arrestment is mainly concentrated in the neighborhood near the fasteners. Therefore, by keeping fastener diameter the same, the wider the specimen, the larger the area that is not affected by the arrestment. Furthermore, it is easier for the crack growth to occur. To better understand the effect of the variation of width on the arrestment, 3-D model should be developed to capture the crack front characteristics.

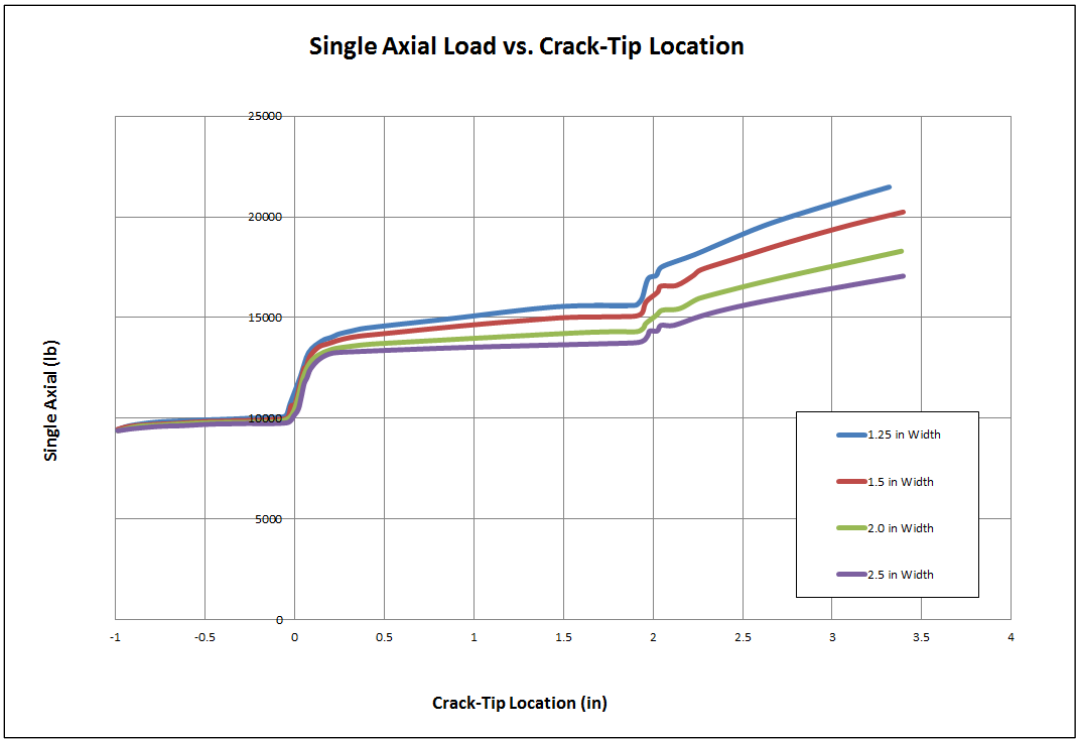

Figure 3.2 Propagation Load for Varying Specimen Width

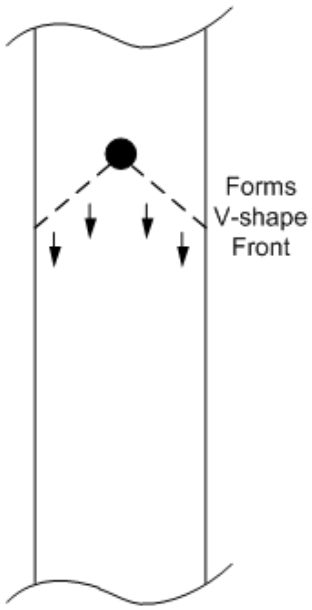

Figure 3.3 Crack Front in Arrested Phase

3.3 Variation of Fastener Spacing

According to AISC Design Provision, the design for fastener spacing should satisfy the following requirements: 1) the minimum distance between the centers of bolts in standard holes shall not be less than three times the diameter of the bolt; 2) For sealing against penetration of moisture in joints, the spacing on a single line adjacent to the free edge shall satisfy $s \le (4.0 + 4.0t) \le 7.0$; 3) The maximum spacing for bolt holes is 24 times the thickness of the thinner plate. In general, in aircraft design, a distance of six to eight times the diameter of the bolt is preferred. In this section, effect of variation of fastener spacing is investigated. The spacing used here is summarized in Table 3.4.

Table 3.4 Fastener Spacing Variation Values

Fastener spacing	Spacing-to-diameter ratio
1.5 in	6
2.0 in	8
2.5 in	10
3.0 in	12

Figure 3.4 shows the effect of varying the fastener spacing from the base configuration. It can be seen from the plot that the fastener spacing does not significantly affect the crack propagation characteristics. The second fastener will not shift the failure mode away from delamination until the crack tip reaches it. Thus, without consideration of the maximum allowable crack length, the distance the arrest fastener in laminated composite structures could be chosen arbitrarily.

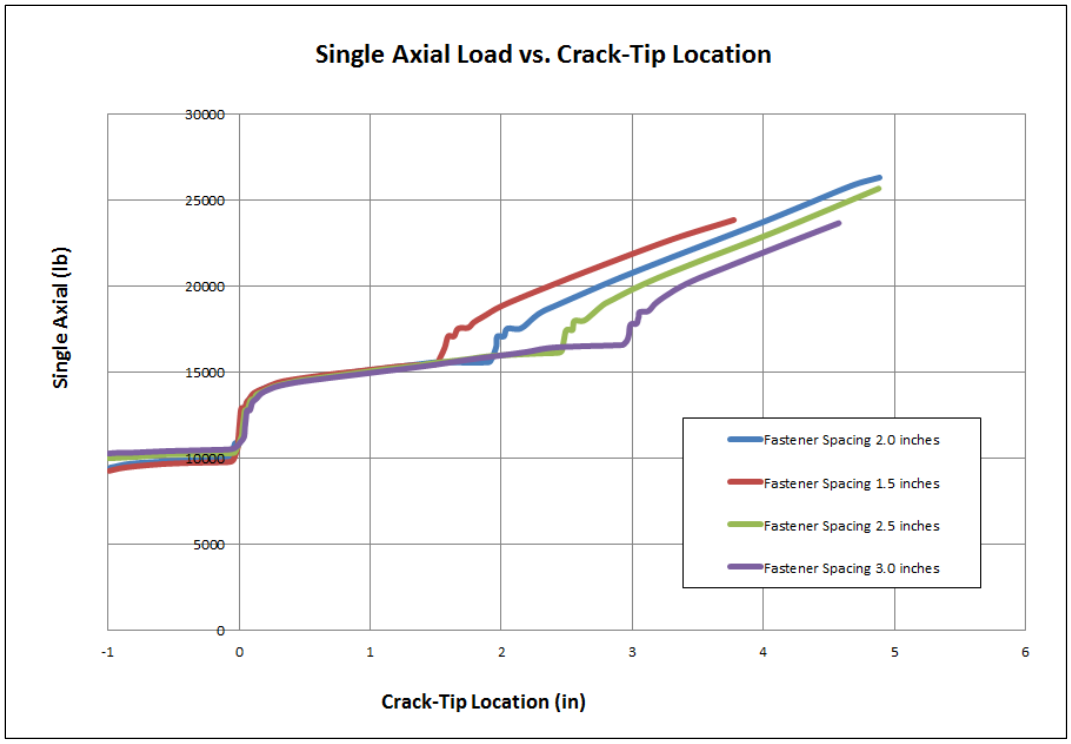

Figure 3.4 Propagation Load for Varying Fastener Spacing

3.4 Variation of G_{IIC}

The fracture toughness is a property which describes the ability of a material containing a crack to resist fracture, and is one of the most important properties of any material for many design applications. If the strain energy release rate exceeds a critical value G_c, then the crack will grow spontaneously. In this section, effect of variation of fracture toughness on crack propagation load is investigated. In general, total fracture toughness can be decomposed into three modes: G_{IC}, G_{IIC}, and G_{IIIC} (which is not our concern due to 2-D modeling). In a manufacturing environment, G_{IIC} is much easier to be controlled than G_{IC}. Therefore, the fracture toughness between the laminates was varied by only selecting different values of G_{IIC}, with holding G_{IC} constant. Table 3.5 describes the variations in G_{IIC}.

Table 3.5 Fracture Toughness Variation Values

G_{IC} (lb*in/in^2)	G_{IIC} (lb*in/in^2)	G_{IC} -to- G_{IIC} Ratio
1.6	14	0.114
1.6	10	0.16
1.6	6	0.267
1.6	2	0.8

As shown in Figure 3.5, an increase in G_{IIC} results in an increase in the load required to initiate and propagate the crack. However, it does not significantly affect the effectiveness of crack arrestment for fasteners. As seen in the plot, the curve shifts up in vertical direction with G_{IIC} increasing. Fracture toughness is a property of material. It drives the propagation load to be increased globally. This conclusion is only valid when G_{IIC} changes itself, with G_{IC} keeping unchanged. This is because Mode I is shut down when the crack past the fastener, while Mode II always exists.

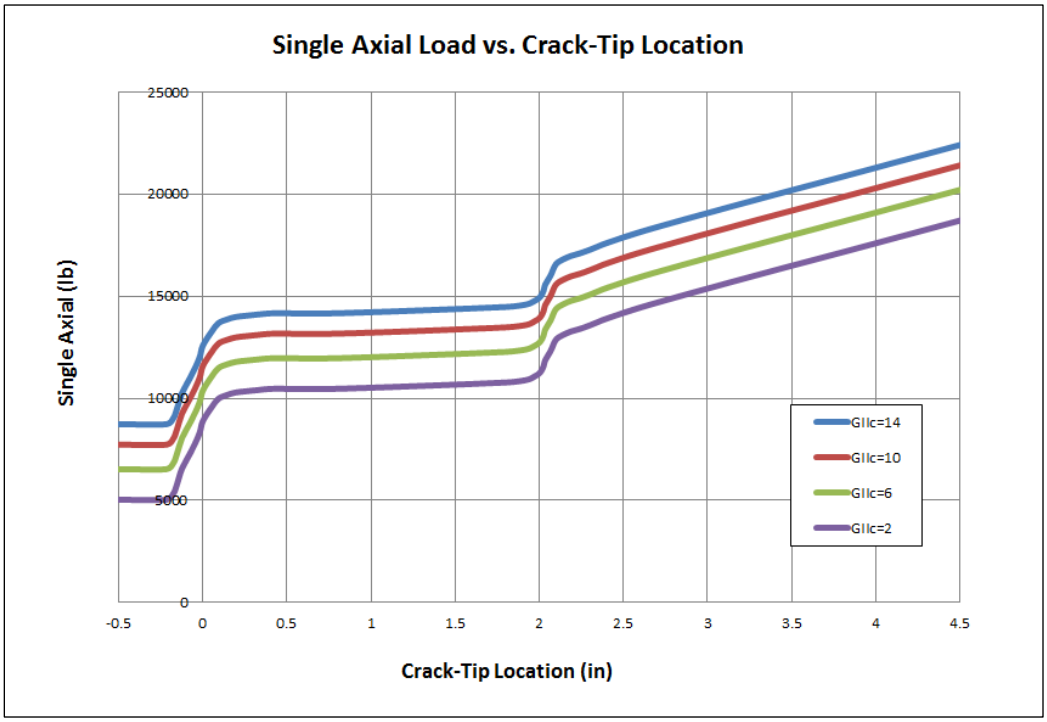

Figure 3.5 Propagation Load for Varying G_{IIC}

3.5 Variation of Fastener Properties

Since it is the fastener that provides disbond/delamination arrest mechanisms in bonded composite structures, the properties of fastener must be the most important of the factors that determine the effectiveness of the arrest mechanism. The fastener properties investigated in this section include: 1) preload; 2) axial stiffness; 3) shear stiffness. They were varied separately, but both fasteners were conservatively assumed to be kept identical. Table 3.6 summarizes the variations of the parameters.

Table 3.6 Fastener Properties Variation Values

Fastener property	Half value	Reference value	Double value
Preload	1800 lb	3600 lb	7200 lb
Axial stiffness	1.12×10^{6} lb/in	2.25×10^{6} lb/in	4.50×10^{6} lb/in
Shear stiffness	8.04×10^{4} lb/in	1.61×10^{5} lb/in	3.22×10^{5} lb/in

Figure 3.6 demonstrates the results of varying install preload and fastener stiffness. It can be seen clearly that the shear stiffness of the fastener affects the delamination arrestment characteristics significantly. An increase in fastener shear stiffness results in higher load step in the "arrested phase" and more stable crack propagation in the "stable propagation phase" at the location of both the first and the second fastener. The reason for this is that the more shear stiffness the fastener has, the more load the fastener transfers from the lower plate to the upper plate, which reduces the load transferred at the crack tip. Varying install preload and axial stiffness of the fastener have only a limited effect; and this effect was only captured in the "arrested phase". It does not affect the "stable propagation phase" at all. To some degree, doubling the axial stiffness of the fastener is equivalent to halving the install preload. Both of them lead to a slight decrease in load step at the location of the fasteners. In conclusion, therefore, the shear stiffness/compliance of the fastener is the key to determine the arrest capability of the fasteners.

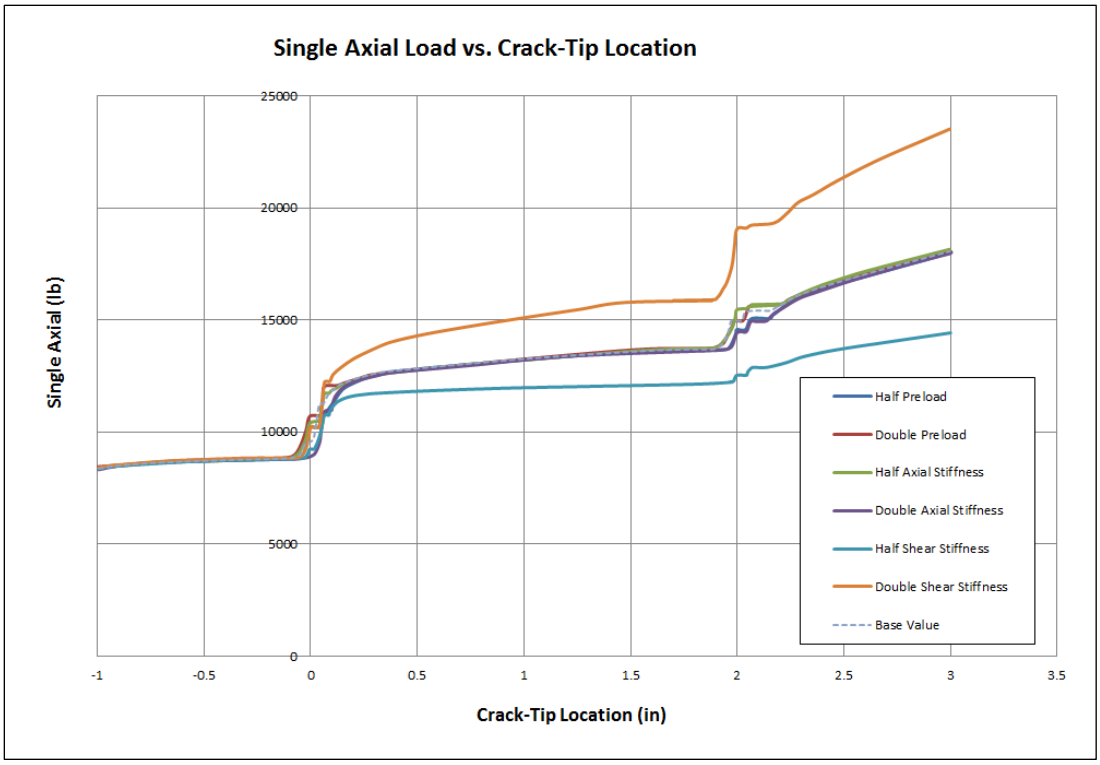

Figure 3.6 Propagation Load for Varying Fastener Properties

3.6 Influence of Friction

Crack face friction is a common issue encountered in Mode II specimen such as the End Notched Flexure (ENF). However, the crack arrest feature discussed here is instead a major source of friction due to the install preload of the fastener. In order the accurately predict the crack arrest behavior in the arrested phase, the crack-face friction must be well-understood. Install preload used in structure assemblies could be a significant fraction of the tension yield load of the fastener, resulting in friction that is orders of magnitude greater than that between a pair of otherwise unloaded crack faces. This means the influence of friction must be investigated. To simulate the effect of friction, the mixed-mode load case as above is still used. A constant fastener preload of 3600 lb is applied and the crack-face static coefficient of friction is varied from zero to 0.75.

Figure 3.7 illustrates the influence of crack face friction. The step increase in propagation load at the location of the first fastener due to mode transition occurs more than 0.2 inches before the crack tip reaches the fastener, due to the elastic influence of the fastener generated by the preload. The second fastener has this elastic influence area, as well; but it is much smaller. Contact friction, together with the fastener install preload, play an important role in arresting crack propagation in Mode II. The existence of friction reduces the load transferred by the crack tip and increases the propagation load as a result.

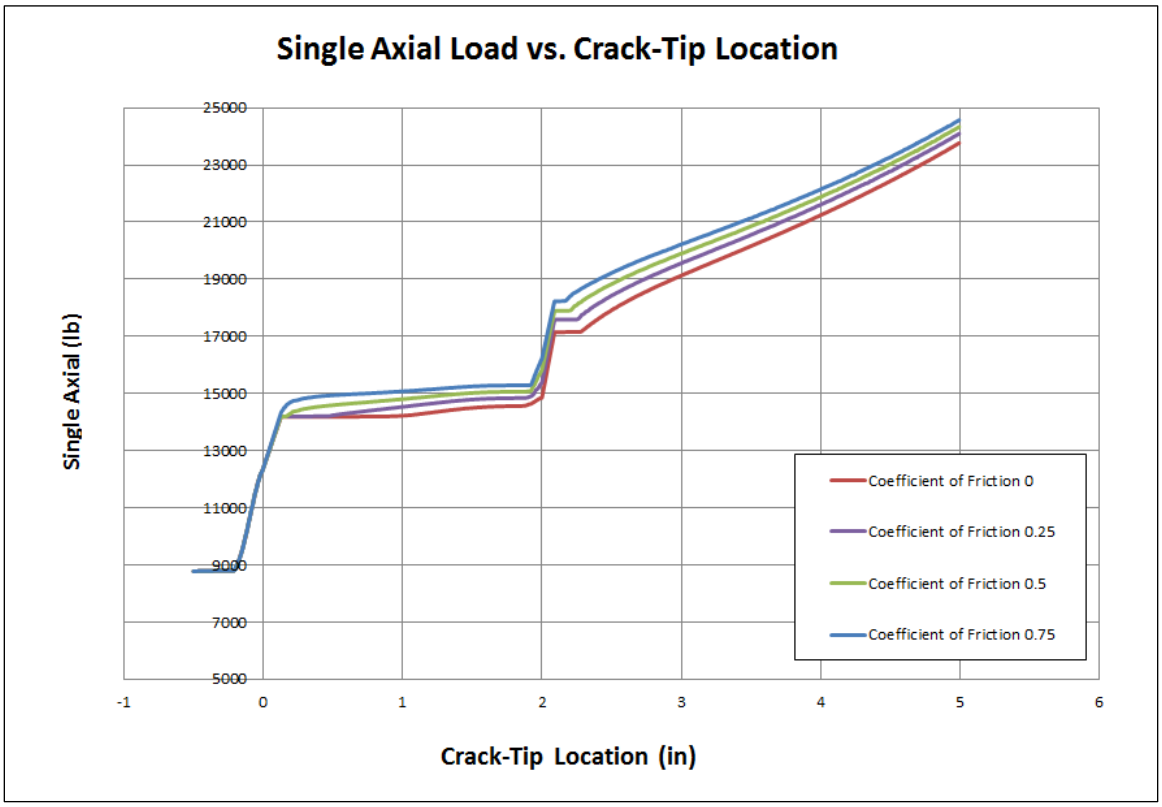

Figure 3.7 Influence of Crack Face Friction

Chapter 4

SUMMARY AND CONCLUSIONS

Analysis of effectiveness of fasteners installed in series as crack arrest features in composite structures has been demonstrated in the finite element code, Abaqus, and experimentally verified. In the finite element model, in conjunction with the experimental testing, it is shown that the presence of fasteners is highly effective in arresting the propagation of a crack via three main mechanisms: 1) mode I suppression, 2) crack-face friction, and 3) fastener joint stiffness. Mechanisms 1) and 2) provide the benefit seen in the arrested phase, while mechanism 3) provides the benefit in the stable propagation phase. The parameters dictating the performance of mechanisms 2) and 3) are structural parameters, e.g. fastener size, install torque, laminate layups. The performance of mechanism 1) is primarily dependent upon the amount of G_I present; in a pure Mode II case, and a conservative assumption of frictionless crack-face is used, one could expect this mechanism would provide no benefit to crack arrestment.

It is also indicated that effectiveness of the first arrest fastener is primarily provided by mechanism 1) and 2). The effectiveness of the second arrest fastener is primarily provided by mechanism 2) and 3). This is because the initial crack begins to propagate under mixed mode condition and the presence (even a small amount) of G_I is significantly more dangerous for the safety of integrated structures compared to G_{II} . The first fastener is extremely effective in eliminating G_I by restricting the opening displacement around the crack tip, forcing the crack into pure Mode II propagation. The propagation load subsequently increases, achieving the desired effect of crack arrestment. In contrast, since pure Mode II load becomes the only factor that drives the crack to continue going down after the crack tip passes the first fastener, the fracture mode transition is no longer exist at the location of the second fastener, that is, mechanism 1) provides no benefit. At the same time, mechanism 3) becomes the dominant arrestment mechanism due to the beneficial superposition of joint stiffness between the two fasteners, which makes the crack propagation more stable.

A two dimensional finite element modeling method is developed in Abaqus which determines the crack propagation load using VCCT elements. The FE analysis predicts similar behavior as the experimental results. Based on this FE model, a series of parametric study were performed. The following parameters were varied: laminate stiffness, laminate width, fastener spacing, fastener stiffness, G_{IIC} of the bond, coefficient of friction on crack-face. The results of parametric study indicated that the disbond/delamination arrestment in bolted bonded composite structures is enhanced by increasing the laminate stiffness, fastener stiffness, coefficient of friction, and interface toughness. Decreasing the specimen width is also of help.

Although the experimental results generally agree with the analytical prediction, some discrepancies can still be observed. The error can be due to the deficit in the understanding and certainty of some parameters with significant influence on the arrest capability of the fasteners, which prompts for more research to understand this important part of the arrest feature. One particularly important area for further study is the crack-face friction. However, parameters affecting it, such as fastener preload and crack-face coefficient of friction are notoriously difficult to predict, measure, or control. It is noted that coefficient of friction is not a material property. In particular, crack-face friction is dependent on the fiber directions bounding the interface, and changes under fatigue loading. Fastener preload cannot be directly controlled. Fastener installation standards only specify install torque, which is measurable during the installation process. The installation torque cannot be reliably related to the generated bearing pressure without experimental characterization of the fastener in question. Another area of further study is the shear stiffness of the fastener joint. Traditional fastener flexibility approaches, proposed by Huth, were usually used for bearing-bypass analysis of arrayed bolted/riveted-joints. It cannot provide accurate descriptions of the behavior of the fastener joint in an arrest configuration.

Furthermore, other failure modes, including laminate failure, fastener yield, fastener pull-through and joint bearing failure, are not considered in this study. A proper design of such crack arrest mechanism should take into account all other failure modes.

In general, the presence of fasteners or fastener-like crack arrest features will turn a potentially-catastrophic unstable crack propagation into a stable one, providing fail-safety to the composite structure. As all the parameters discussed in the last paragraph are more fully understood, it is expected that the model and experimental results will further converge; and the finite element analysis tool could be used in the design environment.

LIST OF REFERENCES

[1] Bruun, E.D., Cheung, C.H., and Lin, K.Y., "Design and Experimental Validation of a Mixed Mode Crack Arrest Specimen," 53rd AIAA SDM Conference, Honolulu, HI, April 2012

[2] Cheung, C.H., Bruun, E.D. and Lin, K.Y., "Design and Optimization of an Axial Mode II Crack Arrest Specimen," 53rd AIAA SDM Conference, Honolulu, HI, April 2012

[3] Cheung, C.H., Gray, P.G., and Lin, K.Y., "Fastener as Fail-Safe Disbond/Delamination Arrest for Laminated Composite Structures," 18th International Conference on Composite Materials (ICCM18), Jeju Island, Korea, August 21-26, 2011

[4] A. C. GARG, "Delamination - A Damage Mode in Composite Structures," Eng. Fracture Mech., Vol. 29, pp. 557-584, 1988.

[5] V. V. BOLOTIN, "Delaminations in composite structures: its origin, buckling, growth and stability," Composites Part B: Engineering, Vol. 27B, pp. 129-145, 1996.

[6] N. J. PAGANO AND G. A. SCHOEPPNER, Delamination of Polymer Matrix Composites: Problems and Assessment, in Comprehensive Composite Materials, Vol. 2, A. Kelly and C. Zweben, Eds.: Elsevier Science Ltd., 2000, pp. 433-528.

[7] T. K. O'BRIEN, Characterization of Delamination Onset and Growth in a Composite Laminate, in Damage in Composite Materials, ASTM STP 775, 1982, pp. 140-167.

[8] T. K. O'BRIEN, Interlaminar fracture toughness: The long and winding road to standardization,Composites Part B, Vol. 29, pp. 57-62, 1998.

[9] R. H. MARTIN, Incorporating interlaminar fracture mechanics into design, in International conference on Designing Cost-Effective Composites: IMechE Conference Transactions, London, U.K., 1998, pp. 83-92.

[10] R. Krueger, "The Virtual Crack Closure Technique: History, Approach and Applications," NASA/CR-2002-211628, CAICASE Report No. 2002-10

[11] G. R. IRWIN, Fracture I, in Handbuch der Physik VI, Flügge, Ed., 1958, pp. 558-590.

[12] D. BROEK, "Elementary Engineering Fracture Mechanics," 4th revised ed: Kluwer Academic Publishers, 1991.

[13] E. F. Rybicki, M. F. Kanninen, "A Finite Element Calculation of Stress Intensity Factors by a Modified Crack Closure Integral," Engineering Fracture Mechanics, Vol. 9, pp. 931-938,1977

[14] G. E. Mabson, L. R. Deobald, B. Dopker, "Fracture Interface Elements for the Implementation of the Virtual Crack Closure Technique," 48th AIAA/ ASME/ ASCE/ AHS/ ASC Structures, Structural Dynamics, and Materials Conference, Honolulu, Hawaii, 23rd-26th April, 2007

[15] Q. Qian and D. Xie, "Analysis of Mixed-Mode Dynamic Crack Propagation by Interface Element Based on Virtual Crack Closure Technique," Engineering Fracture Mechanics, Vol. 74, pp. 807-814, 2007

[16] Z. Suo and J. W. Hutchinson, "Interface Crack between Two Elastic Layers," International Journal of Fracture, Vol. 43, pp. 1-18, 1990

[17] J. L. Wang, "Mechanics and Fracture of Hybrid Material Interface bond," Ph.D. Dissertation, Department of Civil Engineering, The University of Akron, OH, USA.

[18] G. Morris, "Defining a Standard Formula and Test-Method for Fastener Flexibility in Lap Joints," Ph.D. Thesis, TU Delft, April, 2004.

[19] Tate, M.B. and Rosenfeld, S.J., "Preliminary Investigation of Loads Carried by Individual Bolts in Bolted Joints," Technical Note No. 1051, National Advisory Committee of Aeronautics, 1984

[20] H. Huth "Influence of Fastener Flexibility on the Prediction of Load Transfer and Fatigue Life for Multiple-Row Joints," Fatigue in Mechanically Fastened Composite and Metallic Joints, ASTM STP 927, 1986, pp. 221-250.

[21] A. Rutman and J. B. Kogan, "Multi-Spring Representation of Fasteners for MSC/Nastran Modeling," Proceeding of the First MSC Conference for Aerospace Users, Los Angeles, CA, 1997.

[22] L. J. Hart-Smith, "Design Methodology for Bonded-Bolted Composite Joints," Technical Report AFWAL-TR-81-3154, Douglas Aircraft Company, 1982.

[23] G. Kelly, "Quasi-static Strength and Fatigue Life of Hybrid Bonded/bolted Composite Single-lap Joints," Journal of Composite Structures, Vol. 72, pp. 119-129, 2006.

[24] A. Barut and E. Madenci, "Analysis of Bolted-Bonded Composite Single-lap Joints Under Combined In-plane and Transverse Loading," Composite Structures, Vol. 88, pp. 579-594, 2009.